

Pulse Shaping Filter Design for Integrated Sensing & Communication with Zak-OTFS

Nishant Mehrotra*

Electrical and Computer Engineering
Duke University
Durham, USA
nishant.mehrotra@duke.edu

Sandesh Rao Mattu*

Electrical and Computer Engineering
Duke University
Durham, USA
sandesh.mattu@duke.edu

Robert Calderbank

Electrical and Computer Engineering
Duke University
Durham, USA
robert.calderbank@duke.edu

Abstract—Zak-OTFS is an emerging framework for integrated sensing & communication (ISAC) in high delay and Doppler spread environments. A critical enabler for ISAC with Zak-OTFS is the design of pulse shaping filters. For sensing, a localized pulse shaping filter enables ideal input-output (I/O) relation estimates close to the physical scattering channel. For communication, orthogonality of the pulse shape on the information lattice prevents inter-symbol interference, and no time and bandwidth expansion enables full spectral efficiency. A filter simultaneously meeting all three objectives is ideal for ISAC. Existing filter designs achieve two of the above objectives, but not all three simultaneously. For instance, the sinc filter is orthogonal and bandwidth/time-limited, but is not localized. The Gaussian filter is localized and bandwidth/time-limited, but not orthogonal. The RRC filter is localized and orthogonal, but not bandwidth/time-limited. A recently proposed hybrid Gaussian-sinc filter is more localized than the sinc filter and bandwidth/time-limited, but is not orthogonal. In this work, we design optimal pulse shaping filters meeting all three objectives via the Isotropic Orthogonal Transform Algorithm. The proposed pulse shaping filters offer improved data detection (communication) and I/O relation estimation (sensing) performance compared to existing filter choices in the literature.

Index Terms—6G, Equalization, Integrated Sensing and Communication, Pulse Shaping, Zak-OTFS

I. INTRODUCTION

ZAK-OTFS (orthogonal time frequency space modulation) [1]–[3] is an emerging framework for communications and radar sensing in doubly selective channels with high delay and Doppler spreads. The Zak-OTFS carrier waveform is a pulse in the delay-Doppler (DD) domain, formally a quasi-periodic localized function termed *pulsone* with specific periods along delay and Doppler. When the pulsone’s delay period exceeds the channel delay spread and the pulsone’s Doppler period exceeds the channel Doppler spread, the Zak-OTFS Input/Output (I/O) relation changes slowly and predictably, and does not fade [1]–[3]. This non-fading behavior of Zak-OTFS makes it well-suited for high rate communications in extreme mobility scenarios, such as on

This work is supported by the National Science Foundation under grants 2342690 and 2148212, in part by funds from federal agency and industry partners as specified in the Resilient & Intelligent NextG Systems (RINGS) program, and in part by the Air Force Office of Scientific Research under grants FA 8750-20-2-0504 and FA 9550-23-1-0249.

* denotes equal contribution.

TABLE I: Comparison of different DD pulse shaping filters.

Filter	Sidelobe Level	Orthogonal?	Time/BW Limited?
Sinc [1]–[5]	High	✓	✓
RRC [1]–[7]	Low	✓	×
Gaussian [5]	None	×	✓
Gaussian-sinc [8]	Low	×	✓
IOTA (Proposed)	Low	✓	✓

bullet trains, where legacy time-frequency modulations, such as orthogonal frequency division multiplexing (OFDM), fail. Moreover, the response to a single Zak-OTFS carrier provides an image of the scattering environment, which can be used to predict the I/O response to all other carriers. The image of the scattering environment supports sensing in systems such as passive radars that integrate sensing and communications [2].

In its original form, the DD pulsone occupies infinite time and bandwidth. For practical implementation, the DD pulsone is limited to a finite time interval T and bandwidth B via DD domain filtering with a *pulse shaping filter* [1]–[8]. Subsequently, BT information symbols are mounted on DD pulsones shifted by multiples of the delay resolution $1/B$ and Doppler resolution $1/T$. An ideal pulse shaping filter must satisfy three objectives: (i) localization to enable accurate I/O relation estimation (sensing), (ii) orthogonality on the information lattice to prevent inter-symbol interference, and (iii) no time and bandwidth expansion beyond B and T to achieve full spectral efficiency. A filter simultaneously meeting all three objectives is ideal for both sensing and communication.

Previous works on Zak-OTFS utilize standard analytical pulse shaping filters, such as sinc [1]–[5], root raised cosine (RRC) [1]–[7] and Gaussian [5], which meet two but not all three objectives simultaneously. For instance, the sinc filter has the advantage of being orthogonal to shifts by multiples of the delay and Doppler resolution where information symbols are mounted. This property results in excellent data detection (communication) performance assuming the I/O relation is known perfectly. In the absence of perfect I/O relation knowledge, however, the high sidelobes of the sinc filter result in high I/O relation estimation (sensing) error, thus degrading practical data detection performance [1]–[5]. The RRC filter overcomes the high sidelobe drawback of the sinc filter at the

cost of bandwidth and time expansion beyond B and T [1]–[7], making it less suitable for practical implementation. The Gaussian filter has the advantage of being maximally localized in the DD domain – enabling excellent I/O relation estimation (sensing) – however, is not orthogonal to shifts by multiples of the delay and Doppler resolution [5] and thus has poor data detection performance.

Recent work [8] utilizes the (normalized) product of the Gaussian and sinc filters, termed the *Gaussian-sinc* filter, to retain the complementary strengths of the Gaussian and sinc filters with no bandwidth or time expansion. The filter has lower sidelobes and is more localized than the sinc filter, enabling accurate I/O relation estimation and good data detection performance simultaneously. However, the Gaussian-sinc filter is not orthogonal to shifts by multiples of the delay and Doppler resolution, making it a sub-optimal choice.

In this paper, we design optimal DD pulse shaping filters using the Isotropic Orthogonal Transform Algorithm (IOTA)¹, which has been extensively utilized in time-frequency multicarrier modulations (e.g., filterbank multicarrier) [10]–[13]. We consider two maximally localized² prototype pulse shapes – Gaussian and the prolate spheroidal wave function (PSWF) [14], [15] – and orthogonalize them to shifts by multiples of the delay and Doppler resolution via the IOTA procedure. In Section IV, we show that the proposed pulse shaping filters offer improved data detection and I/O relation estimation performance over the Gaussian-sinc filter from [8] since the latter is not orthogonal. Table I places our contributions in the context of prior work.

Notation: x denotes a complex scalar, \mathbf{x} denotes a vector with n th entry $\mathbf{x}[n]$, and \mathbf{X} denotes a matrix with (n, m) th entry $\mathbf{X}[n, m]$. $(\cdot)^*$ denotes complex conjugate, $(\cdot)^\top$ denotes transpose, $(\cdot)^\text{H}$ denotes complex conjugate transpose. Calligraphic font \mathcal{X} denotes operators or sets, with usage clear from context. $|\cdot|$ denotes set cardinality or absolute value, with usage clear from context. \mathbb{Z} denotes the set of integers and \mathbb{Z}_N the set of integers modulo N . $\delta(\cdot)$ denotes the delta function, and \mathbf{I}_N denotes the $N \times N$ identity matrix.

II. OVERVIEW OF ZAK-OTFS

We provide a brief overview of Zak-OTFS in this Section, and refer the interested reader to [1]–[3] for a more detailed description of Zak-OTFS.

The Zak-OTFS carrier waveform is a pulse in the delay-Doppler (DD) domain, formally a quasi-periodic localized function termed the *DD pulsone*. The DD pulsone is characterized by a delay period τ_p and a Doppler period ν_p , with $\tau_p \nu_p = 1$. The DD pulsone located at delay τ_0 and Doppler ν_0 , where $0 \leq \tau_0 < \tau_p$, $0 \leq \nu_0 < \nu_p$, is given by [1]–[3]:

$$\mathbf{p}_{(\tau_0, \nu_0)}(\tau, \nu) = \sum_{n, m \in \mathbb{Z}} e^{j2\pi n \nu \tau_p} \delta(\tau - n\tau_p - \tau_0) \times \delta(\nu - m\nu_p - \nu_0). \quad (1)$$

¹while possible, we do not consider the alternate approach of Hermite pulse shapes [9]–[11] whose performance remains similar to IOTA pulse shapes [10]

²satisfying Heisenberg’s Uncertainty Principle [10], [13]–[15]

The DD pulsone in (1) occupies infinite time and bandwidth. For practical implementation, the DD pulsone is limited to a time interval T and a bandwidth B via DD domain filtering with a pulse shaping filter $\mathbf{w}(\tau, \nu)$ [1]–[3]:

$$\mathbf{p}_{(\tau_0, \nu_0)}^{\mathbf{w}}(\tau, \nu) = \mathbf{w}(\tau, \nu) *_{\sigma} \mathbf{p}_{(\tau_0, \nu_0)}(\tau, \nu), \quad (2)$$

where $*_{\sigma}$ denotes twisted convolution³.

We mount $BT = MN$ information symbols on the pulse shaped pulsone in (2) at $M = \tau_p/1/B = B\tau_p$ distinct locations along delay and $N = \nu_p/1/T = T\nu_p$ distinct locations along Doppler. Specifically, information symbols are mounted on the lattice $\Lambda = \{(\tau_0, \nu_0) = (k_0/B, l_0/T) : k_0 \in \mathbb{Z}_M, l_0 \in \mathbb{Z}_N\}$ as:

$$\mathbf{x}_{\text{DD}}^{\mathbf{w}}(\tau, \nu) = \sum_{k_0=0}^{M-1} \sum_{l_0=0}^{N-1} \mathbf{X}[k_0, l_0] \mathbf{p}_{(k_0/B, l_0/T)}^{\mathbf{w}}(\tau, \nu), \quad (3)$$

where \mathbf{X} denotes the $M \times N$ array of information symbols.

Note that from (2), we may equivalently express (3) as:

$$\mathbf{x}_{\text{DD}}^{\mathbf{w}}(\tau, \nu) = \mathbf{w}(\tau, \nu) *_{\sigma} \mathbf{x}_{\text{DD}}(\tau, \nu), \quad (4)$$

in terms of an infinite time and bandwidth signal $\mathbf{x}_{\text{DD}}(\tau, \nu)$:

$$\mathbf{x}_{\text{DD}}(\tau, \nu) = \sum_{k_0=0}^{M-1} \sum_{l_0=0}^{N-1} \mathbf{X}[k_0, l_0] \mathbf{p}_{(k_0/B, l_0/T)}(\tau, \nu). \quad (5)$$

After pulse shaping, the time domain (TD) representation of the signal $\mathbf{x}_{\text{DD}}^{\mathbf{w}}(\tau, \nu)$, generated via the inverse Zak transform⁴, is transmitted. Let $\mathbf{h}_{\text{phy}}(\tau, \nu) = \sum_{i=1}^P h_i \delta(\tau - \tau_i) \delta(\nu - \nu_i)$ denote the DD representation of a scattering environment with P paths. The received signal in the DD domain is [1]–[3]:

$$\mathbf{y}_{\text{DD}}(\tau, \nu) = \mathbf{h}_{\text{phy}}(\tau, \nu) *_{\sigma} \mathbf{x}_{\text{DD}}^{\mathbf{w}}(\tau, \nu) + \mathbf{n}_{\text{DD}}(\tau, \nu), \quad (6)$$

where $\mathbf{n}_{\text{DD}}(\tau, \nu)$ denotes the additive noise at the receiver in the DD domain. The receiver performs matched filtering with the filter $\tilde{\mathbf{w}}(\tau, \nu) = e^{j2\pi\nu\tau} \mathbf{w}^*(-\tau, -\nu)$ to obtain [1]–[3]:

$$\mathbf{y}_{\text{DD}}^{\tilde{\mathbf{w}}}(\tau, \nu) = \tilde{\mathbf{w}}(\tau, \nu) *_{\sigma} \mathbf{y}_{\text{DD}}(\tau, \nu) = \mathbf{h}_{\text{eff}}(\tau, \nu) *_{\sigma} \mathbf{x}_{\text{DD}}(\tau, \nu) + \mathbf{n}_{\text{DD}}^{\tilde{\mathbf{w}}}(\tau, \nu), \quad (7)$$

where the final step follows on substituting (4) in (6). In (7), $\mathbf{h}_{\text{eff}}(\tau, \nu)$ denotes the *effective channel*⁵ that encompasses the effects of the physical scattering environment as well as pulse shaping and matched filtering [1]–[3]:

$$\mathbf{h}_{\text{eff}}(\tau, \nu) = \tilde{\mathbf{w}}(\tau, \nu) *_{\sigma} \mathbf{h}_{\text{phy}}(\tau, \nu) *_{\sigma} \mathbf{w}(\tau, \nu), \quad (8)$$

and $\mathbf{n}_{\text{DD}}^{\tilde{\mathbf{w}}}(\tau, \nu) = \tilde{\mathbf{w}}(\tau, \nu) *_{\sigma} \mathbf{n}_{\text{DD}}(\tau, \nu)$ denotes the noise at the receiver after matched filtering.

Upon sampling on the information symbol lattice Λ , the system model in (7) reduces to [1]–[3]:

$$\mathbf{y}_{\text{DD}}^{\tilde{\mathbf{w}}}[k, l] = \mathbf{h}_{\text{eff}}[k, l] *_{\sigma_d} \mathbf{x}_{\text{DD}}[k, l] + \mathbf{n}_{\text{DD}}^{\tilde{\mathbf{w}}}[k, l], \quad (9)$$

where $\mathbf{a}[k, l] = \mathbf{a}(k/B, l/T)$, $k \in \mathbb{Z}_M, l \in \mathbb{Z}_N$, denotes samples of $\mathbf{a}(\tau, \nu) \in \{\mathbf{y}_{\text{DD}}^{\tilde{\mathbf{w}}}(\tau, \nu), \mathbf{h}_{\text{eff}}(\tau, \nu), \mathbf{x}_{\text{DD}}(\tau, \nu), \mathbf{n}_{\text{DD}}^{\tilde{\mathbf{w}}}(\tau, \nu)\}$ on the lattice Λ , and $*_{\sigma_d}$ denotes discrete twisted convolution⁶.

³ $\mathbf{a}(\tau, \nu) *_{\sigma} \mathbf{b}(\tau, \nu) = \iint \mathbf{a}(\tau', \nu') \mathbf{b}(\tau - \tau', \nu - \nu') e^{j2\pi\nu'(\tau - \tau')} d\tau' d\nu'$

⁴ $\mathbf{a}(t) = \mathcal{Z}^{-1}(\mathbf{a}(\tau, \nu)) = \sqrt{\tau_p} \int_0^{\nu_p} \mathbf{a}(t, \nu) d\nu$

⁵the effective channel approximates the physical channel when all paths are resolvable in delay with bandwidth B and in Doppler with time T

⁶ $\mathbf{a}[k, l] *_{\sigma_d} \mathbf{b}[k, l] = \sum_{k', l' \in \mathbb{Z}} \mathbf{a}[k - k', l - l'] \mathbf{b}[k', l'] e^{j\frac{2\pi}{NT} k'(l - l')}$

Substituting (5) in (9) and vectorizing gives [1]–[3]:

$$\mathbf{y} = \mathbf{H}\mathbf{x} + \mathbf{n}, \quad (10)$$

where \mathbf{y} , \mathbf{x} , \mathbf{n} are $MN \times 1$ vectors with $\mathbf{y}[k+lM] = \mathbf{y}_{\text{DD}}^{\tilde{\mathbf{w}}}[k, l]$, $\mathbf{x}[k+lM] = \mathbf{x}_{\text{DD}}[k, l]$, $\mathbf{n}[k+lM] = \mathbf{n}_{\text{DD}}^{\tilde{\mathbf{w}}}[k, l]$, and \mathbf{H} is an $MN \times MN$ matrix with entries:

$$\begin{aligned} \mathbf{H}[k+lM, k'+l'M] &= \sum_{n,m \in \mathbb{Z}} e^{j\frac{2\pi}{N}nl'} e^{j\frac{2\pi}{MN}(k'+nM)(l-l'-mN)} \\ &\times \mathbf{h}_{\text{eff}}[k-k'-nM, l-l'-mN]. \end{aligned} \quad (11)$$

Assuming the I/O relation (matrix \mathbf{H}) is known, the receiver detects the information symbols \mathbf{x} from \mathbf{y} , e.g., via the minimum mean squared error (MMSE) estimator [3]. To acquire the I/O relation, a known pilot symbol is transmitted in one of three ways: in a frame separate from data [2], embedded into the same frame as data with appropriate guard regions [5], [6], or overlaid on the same frame as data via a mutually unbiased spreading filter [4]. The receiver estimates the sampled effective channel $\mathbf{h}_{\text{eff}}[k, l]$ via the cross-ambiguity between the received symbols and the pilot symbols (see [4] for more details), which is subsequently used to estimate the matrix \mathbf{H} via (11).

III. PULSE SHAPING FILTERS & THEIR DESIGN

In this Section, we first overview existing choices for the DD pulse shaping filter $\mathbf{w}(\tau, \nu)$ in (2), before outlining our proposed framework for DD pulse shaping filter design.

A. Pulse Shaping Filters in the Literature

Existing literature on Zak-OTFS [1]–[8] has considered the following pulse shaping filters.

1) *Sinc* [1]–[5]: The sinc filter is given by:

$$\mathbf{w}(\tau, \nu) = \sqrt{BT} \text{sinc}(B\tau) \text{sinc}(T\nu). \quad (12)$$

2) *RRC* [1]–[7]: The RRC filter is given by:

$$\mathbf{w}(\tau, \nu) = \sqrt{BT} \text{rrc}_{\beta_\tau}(B\tau) \text{rrc}_{\beta_\nu}(T\nu), \quad (13)$$

where $0 \leq \beta_\tau, \beta_\nu \leq 1$ and:

$$\text{rrc}_\beta(x) = \frac{\sin(\pi x(1-\beta)) + 4\beta x \cos(\pi x(1+\beta))}{\pi x(1-(4\beta x)^2)}. \quad (14)$$

When $\beta_\tau = \beta_\nu = 0$, the RRC filter specializes to the sinc filter. However, when $\beta_\tau, \beta_\nu > 0$, there is bandwidth and time expansion beyond B and T to $(1+\beta_\tau)B$ and $(1+\beta_\nu)T$.

3) *Gaussian* [5]: The Gaussian filter is given by:

$$\mathbf{w}(\tau, \nu) = \sqrt{BT} \left(\frac{4\alpha_\tau \alpha_\nu}{\pi^2} \right)^{1/4} e^{-[\alpha_\tau(B\tau)^2 + \alpha_\nu(T\nu)^2]}. \quad (15)$$

When $\alpha_\tau = \alpha_\nu = 1.584$, there is no bandwidth and time expansion beyond B and T .

4) *Gaussian-sinc* [8]: The Gaussian-sinc filter is given by:

$$\begin{aligned} \mathbf{w}(\tau, \nu) &= \sqrt{BT} \Omega_\tau \Omega_\nu \text{sinc}(B\tau) \text{sinc}(T\nu) \\ &\times e^{-[\alpha_\tau(B\tau)^2 + \alpha_\nu(T\nu)^2]}. \end{aligned} \quad (16)$$

When $\alpha_\tau = \alpha_\nu = 0.044$ and $\Omega_\tau = \Omega_\nu = 1.0278$, there is no bandwidth and time expansion beyond B and T .

B. Proposed IOTA Pulse Shaping Design Framework

To overcome the drawbacks of existing pulse shaping filters from Section III-A (see Section I and Table I), we utilize the Isotropic Orthogonal Transform Algorithm (IOTA) [10]–[13] framework to design DD pulse shaping filters. The key idea is to orthogonalize a maximally localized pulse shape to shifts of the lattice points Λ . The resulting pulse constitutes the closest orthogonal pulse shape to the initial maximally localized pulse.

To apply the IOTA procedure, we consider two maximally localized pulses – the Gaussian pulse in (15) and the prolate spheroidal wave function (PSWF) [14], [15]. In 1D, PSWFs are functions that are bandlimited to $[-B'/2, B'/2]$ and are maximally localized within the time interval $[-T'/2, T'/2]$. 1D PSWFs are given by the eigenvectors of the Fredholm integral:

$$\int_{-T'/2}^{T'/2} \text{sinc}(B'(t-t')) \psi_n(t') dt' = \lambda_n \psi_n(t), \quad (17)$$

where $t \in [-T'/2, T'/2]$ and λ_n denotes the eigenvalue. To generate 2D PSWFs in the DD domain, we solve the problem in (17) over delay and Doppler separately. Specifically, along delay, we set $B' = B$, $T' = \tau_p$, $t = \tau$, $t' = \tau'$ to obtain $\psi_n^{\text{del}}(\tau)$. Along Doppler, we set $B' = T$, $T' = \nu_p$, $t = \nu$, $t' = \nu'$ to obtain $\psi_n^{\text{Dop}}(\nu)$. The DD PSWF filter is given by the product $\mathbf{w}(\tau, \nu) = \psi_n^{\text{del}}(\tau) \psi_n^{\text{Dop}}(\nu)$, with $n = 1$ in practice.

Subsequently, we apply the IOTA procedure to the Gaussian and PSWF filters in two stages.

Stage 1: First, the prototype filter (Gaussian or PSWF) is mounted on the information lattice Λ . For a prototype filter $\mathbf{w}_p(\tau, \nu)$, the following $MN \times |\mathcal{T}||\mathcal{V}|$ matrix is formed:

$$\mathbf{G} = \begin{bmatrix} \cdots & \mathbf{w}_p(\tau - 0/B, \nu - 0/T) & \cdots \\ & \vdots & \\ \cdots & \mathbf{w}_p(\tau - k/B, \nu - l/T) & \cdots \\ & \vdots & \\ \cdots & \mathbf{w}_p(\tau - (M-1)/B, \nu - (N-1)/T) & \cdots \end{bmatrix}, \quad (18)$$

where \mathcal{T} denotes the set of delay values and \mathcal{V} denotes the set of Doppler values spanned by the prototype filter $\mathbf{w}_p(\tau, \nu)$.

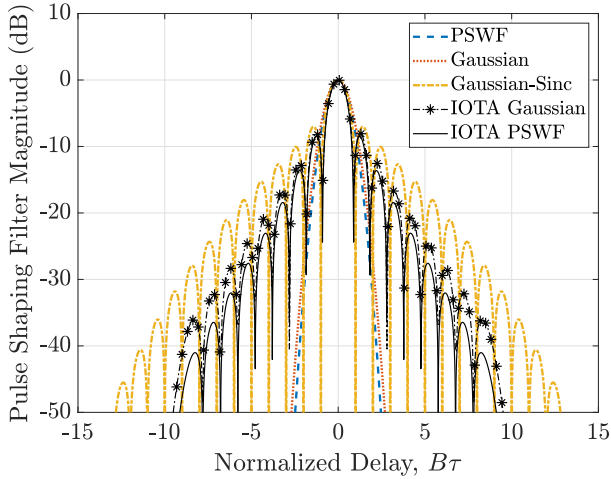
Stage 2: Next, the inter-pulse interference between the MN rows of the matrix \mathbf{G} in (18) is removed, such that the resulting pulses are orthogonal. Let $\mathbf{R} = \mathbf{G}\mathbf{G}^H$ denote the Gram matrix corresponding to \mathbf{G} . The orthogonalized pulses are given by:

$$\tilde{\mathbf{G}} = \mathbf{R}^{-1/2} \mathbf{G}. \quad (19)$$

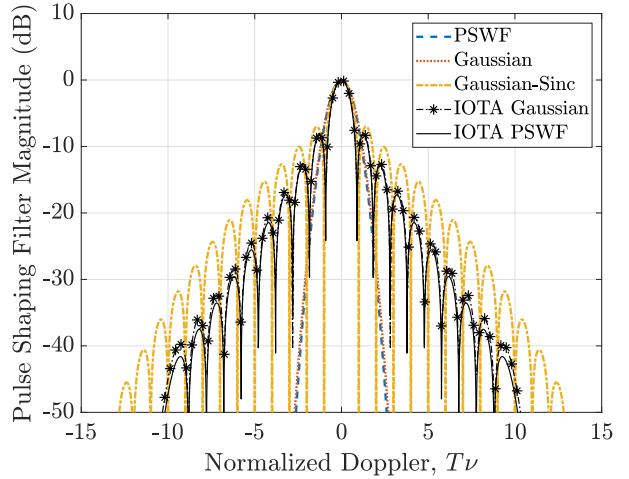
The pulses $\tilde{\mathbf{G}}$ are orthogonal since the corresponding Gram matrix is an $MN \times MN$ identity matrix:

$$\begin{aligned} \tilde{\mathbf{R}} &= \tilde{\mathbf{G}}\tilde{\mathbf{G}}^H \\ &= \mathbf{R}^{-1/2} \mathbf{G}\mathbf{G}^H \mathbf{R}^{-1/2} \\ &= \mathbf{I}_{MN}. \end{aligned} \quad (20)$$

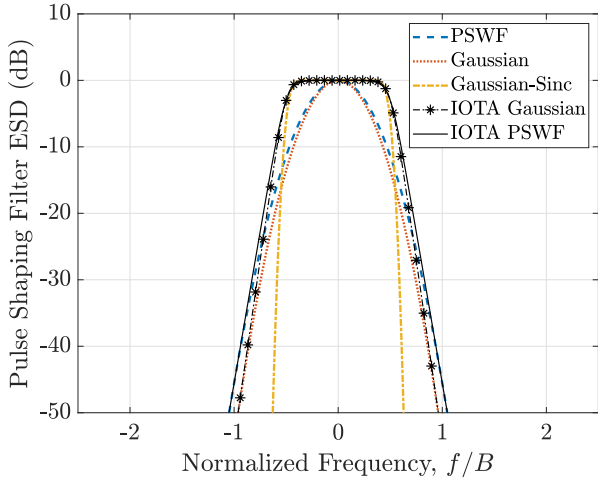
The DD IOTA pulse shaping filter $\mathbf{w}(\tau, \nu)$ corresponds to the first row of $\tilde{\mathbf{G}}$ centered at zero delay and zero Doppler.



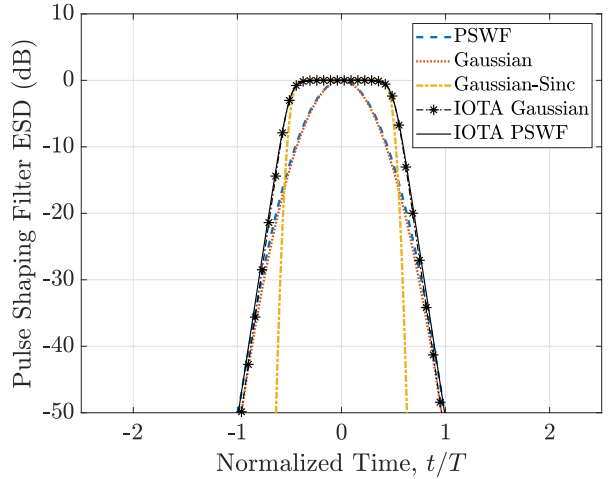
(a) Pulse shaping filter magnitude vs normalized delay.



(b) Pulse shaping filter magnitude vs normalized Doppler.



(c) Energy spectral density (ESD) vs normalized frequency.



(d) Energy spectral density (ESD) vs normalized time.

Fig. 1: Pulse shaping filter variation and energy concentration. (a)-(b): The proposed IOTA pulse shapes have a sharper main lobe and lower sidelobes compared to the Gaussian-sinc filter [8]. Moreover, the IOTA PSWF pulse has smaller main lobe and sidelobes compared to the IOTA Gaussian filter. (c)-(d): The IOTA pulse shapes have flat energy spectral density within $f \in [-B/2, B/2]$ and $t \in [-T/2, T/2]$ and a roll-off similar to their prototype pulses (Gaussian or PSWF). All pulse shapes have 99.99% energy concentration within $f \in [-B/2, B/2]$ and $t \in [-T/2, T/2]$.

TABLE II: Power-delay profile of Veh-A channel model

Path index i	1	2	3	4	5	6
Delay τ_i (μs)	0	0.31	0.71	1.09	1.73	2.51
Relative power (dB)	0	-1	-9	-10	-15	-20

IV. NUMERICAL RESULTS

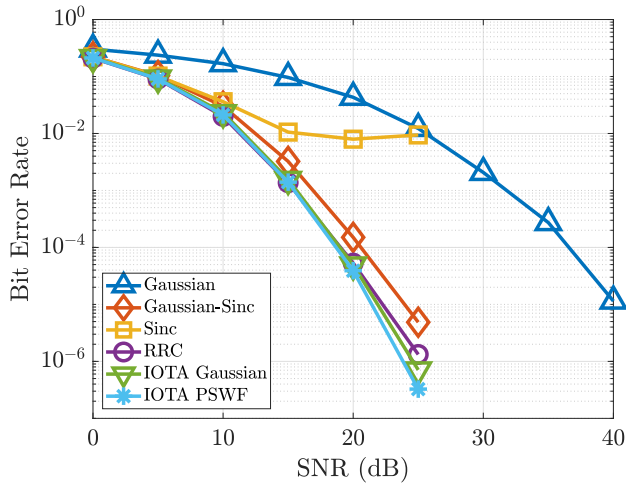
A. Simulation Configuration

We conduct numerical simulations using a 3GPP-compliant $P = 6$ path Vehicular-A (Veh-A) channel model [16] with significant mobility and delay spread, whose power-delay profile is shown in Table II. The Doppler of each path is simulated as $\nu_i = \nu_{\max} \cos(\theta_i)$, with θ_i uniformly distributed in $[-\pi, \pi]$ and $\nu_{\max} = 815$ Hz denoting the maximum channel Doppler

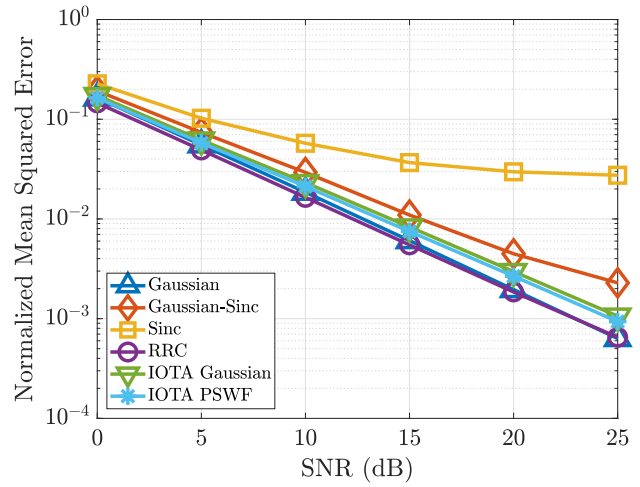
spread. Note that our channel model is representative of real propagation environments since it considers *fractional* delay and Doppler shifts – the path delays in Table II being non-integer multiples of the delay resolution $1/B$, and the Doppler shifts $\nu_i = \nu_{\max} \cos(\theta_i)$ being non-integer multiples of the Doppler resolution $1/T$. We simulate using the parameters: $M = 17, N = 19, \nu_p = 30$ kHz and $\beta_\tau = \beta_\nu = 0.6$ for the RRC filter. While simulations using larger frame sizes and wider bandwidths are possible, they are not pursued since we have shown in [17] that there is no difference in performance.

B. Pulse Shaping Filter Visualization

Fig. 1 visualizes the pulse shaping filter magnitudes and their energy spectral densities (ESD). All pulse shapes have



(a) Bit error rate (BER).



(b) Normalized mean squared error (NMSE).

Fig. 3: Uncoded 4-QAM data detection performance with I/O relation estimation using a separate pilot frame with pilot SNR equal to data SNR. The simultaneous localization and orthogonality of the proposed IOTA pulses results in improved BER and I/O relation NMSE compared to the Gaussian-sinc filter [8], with no time or bandwidth expansion (unlike the RRC filter).

[14] D. Slepian and H. O. Pollak, "Prolate Spheroidal Wave Functions, Fourier Analysis and Uncertainty — I," *The Bell System Technical Journal*, vol. 40, no. 1, pp. 43–63, 1961.

[15] H. J. Landau and H. O. Pollak, "Prolate Spheroidal Wave Functions, Fourier Analysis and Uncertainty — II," *The Bell System Technical Journal*, vol. 40, no. 1, pp. 65–84, 1961.

[16] ITU-R M.1225, "Guidelines for evaluation of radio transmission technologies for IMT-2000," *International Telecommunication Union Radio communication*, 1997.

[17] N. Mehrotra, S. R. Mattu, and R. Calderbank, "Zak-OTFS With Spread Carrier Waveforms," *IEEE Wireless Communications Letters*, vol. 14, no. 10, pp. 3244–3248, 2025.